11th International Workshop on Ship and Marine Hydrodynamics
Hamburg, Germany, September 22-25, 2019

Quantitative Evaluation of Temporal Variation for the Short-Crested Irregular Wave Generated in Experimental Wave Basin

Daichi Ota[1,*], Takako Kuroda[1], Hidetaka Houtani[1, 2]

[1]National Maritime Research Institute
6-38-1, Shinkawa, Mitaka-shi, Tokyo 181-0004, Japan
[2]The University of Tokyo
7-3-1, Hongo, Bunkyo-ku, Tokyo 113-8656, Japan

*Corresponding author, ota-d@nmri.go.jp

ABSTRACT

In a model test aimed at investigating statistically the ship response in an actual sea condition, it is needed that the short-crested irregular waves are generated for a long duration. The characteristics of the wave field should be kept unchanged in time. In this study, the authors have investigated the temporal variation of a short-crested irregular wave field in an experimental wave basin. An experiment of wave generation was carried out in the Actual Sea Model Basin (ASMB) of National Maritime Research Institute in Japan. Wave elevations were measured with six wave gauges to estimate the directional spectrum. In order to evaluate quantitatively the temporal variation of the wave field, the authors introduced the indicators of the wave spectrum shape such as significant wave height, mean wave period, mean wave direction, and mean spreading angle. The authors evaluated the temporal variation of the experimental wave field generated in the ASMB by using these indicators. In addition, the variation of the proposed indicators of the wave spectrum shape due to the development of the reflected wave along with wave generation time was investigated by numerical simulation. The introduction of these wave parameters allowed us to quantify the temporal variation of wave fields.

1 INTRODUCTION

In recent years, time domain simulation tools to predict the ship motions in short-crested irregular waves have been developed (e.g., [1]). These numerical tools should be validated by experimental model tests in short-crested irregular waves. In such model tests, the characteristics of the wave field generated in a wave basin should be kept unchanged for a long duration from the statistical perspective.

Most of the existing wave basins equip wave-makers on only one or adjacent two sides of the basin, but some wave basins install wave-makers around the entire periphery. Experimental wave conditions that can be generated in a wave basin depend on the arrangement of wave-makers. Comprehension of the properties for the waves generated in the wave basin is important. Properties of the wave field generated in a wave basin, whose entire periphery is surrounded by wave-makers, have been investigated. Maeda et al. [2] investigated the temporal variation of the frequency spectrum and the directional spreading function of wave field generated in a circular wave basin. However, the temporal variation of the short-crested irregular wave fields has not been evaluated quantitatively in their study. In this study, the authors have evaluated the temporal variation of the short-crested irregular wave field in an experimental wave basin by introducing the indicators of the wave spectrum shape such as significant wave height, mean wave period, mean wave direction and mean spreading angle.

2 WAVE GENERATION EXPERIMENT

2.1 Facility

Actual Sea Model Basin (ASMB) of National Maritime Research Institute in Japan is fully surrounded by 382 segmented flap-type absorbing wave-makers. The overview and coordinate system of the ASMB are shown in Figure 1. The ASMB is 80m in length, 40m in width and 4.5m in depth and is equipped with towing carriage. The ASMB is capable to carry out the towing test in various wave conditions including short-crested irregular wave [3]. In such a model test, the characteristics of the wave field should be kept unchanged during the measurement of ship response. In order to investigate the temporal variation of the wave field characteristics generated in the ASMB, the authors conducted the experiment of wave generation in the ASMB.

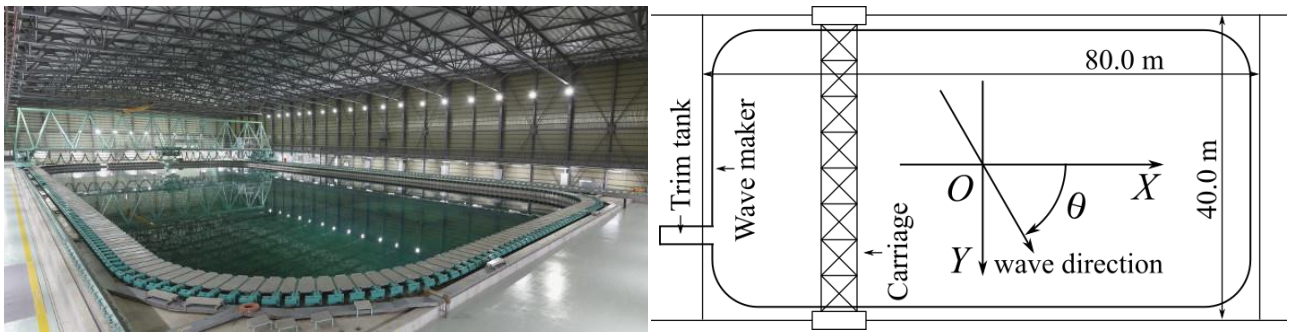

Figure 1: Overview and coordinate system of the ASMB.

2.2 Experimental method

In the experiment of wave generation, a short-crested irregular wave was generated. The wave condition is shown in Table 1. The frequency spectrum $S(f)$ of the experimental wave is ISSC spectrum as represented in Eq. (1). Significant wave height $H_{1/3}$ and mean wave period T_{01} are used as the parameters of the ISSC spectrum. In the wave generation experiment, the surface elevation of the generated wave $\zeta(x, y, t)$ is expressed by the single summation method (e.g., [4]). In the single summation method, the surface elevation is represented as a linear superposition of the component waves as Eq. (2). Moreover, each component wave direction corresponds to one frequency component, respectively. The cosine-4 spreading function as expressed in Eq. (3) is used for the distribution of the component wave directions in the experiment.

Table 1: Condition of short-crested irregular wave in model scale.

Frequency spectrum model	ISSC spectrum
Significant wave height $H_{1/3}$ (cm)	5.73
Mean wave period T_{01} (s)	1.05
Directional spreading function	Cosine-4
Principal wave direction θ_p (deg)	90.0

$$S(f) = 0.11 H_{1/3}^2 T_{01}^{-4} f^{-5} \exp(-0.44 T_{01}^{-4} f^{-4}) \tag{1}$$

$$\zeta(x, y, t) = \sum_{i}^{N} a_i \cos(k_i x \cos\theta_i + k_i y \sin\theta_i - 2\pi f_i t + \varepsilon_i) \tag{2}$$

where:

a_i	wave amplitude of frequency component
k_i	wavenumber of component
ε_i	initial phase angle of component

$$G(\theta) = \begin{cases} G_0 \cos^4(\theta - \theta_p), & |\theta - \theta_p| \le \frac{\pi}{2} \\ 0 \quad , & |\theta - \theta_p| > \frac{\pi}{2} \end{cases} \tag{3}$$

where:

G_0 normalization factor

The short-crested irregular wave was generated for 20-minutes. The surface elevation was measured during the wave generation by wave gauge array as shown in Figure 2. Six wave gauges were arranged in a regular pentagonal shape with a distance of 0.2 m from the center to each vertex. That layout follows the wave gauge arrangement criteria proposed by Goda [4] as follows; "1) No pair of wave gauges should have the same vector distance between gauges. 2) The vector distance should be distributed uniformly in as wide a range as possible. 3) The minimum separation distance between a pair of wave gauges should be less than one half of the smallest length of the component waves for which the directional analysis is to be made."

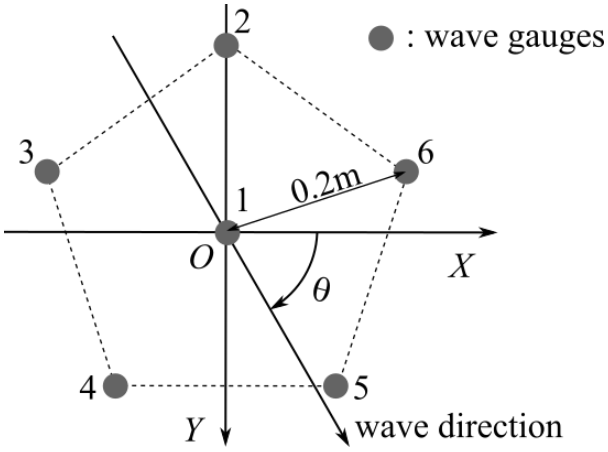

Figure 2: Arrangement of wave gauge array.

3 ANALYSIS METHOD AND RESULTS OF THE EXPERIMENTAL WAVE FIELD

3.1 Analysis method of the experimental wave field

In order to evaluate quantitatively the temporal variation of the short-crested irregular wave generated in the experiment, temporal variations of the directional wave spectrum shapes were investigated. In the analysis of the experimental result, the time series of the surface elevations for 20-minutes were divided into four 5-minutes intervals. In each interval, the frequency spectra $S(f)$ were estimated using the fast Fourier transform (FFT), and the directional spectra $S(f,\theta)$ were estimated by the extended maximum entropy principle (EMEP) method [5] as follows.

The cross-spectrum $\Phi_{mn}(f)$ for a pair of surface elevations measured at two different locations (x_m, y_m) and (x_n, y_n) is expressed using the directional spectrum $S(f,\theta)$ as Eq. (4) [6]. Here, we express the directional spectrum $S(f,\theta)$ as a product of the frequency spectrum $S(f)$ and the directional spreading function $G(\theta)$ as Eq. (5). In the EMEP method, the directional spreading function $G(\theta)$ is assumed to be expressed as Eq.(6) including parameters a_0, a_n and b_n. These parameters are determined from the cross-spectra of the measured surface elevations by using Eq. (4) such that the entropy is maximized (see [5]). Eventually, the directional spectrum $S(f,\theta)$ is obtained as Eq. (5) using the estimated frequency spectrum $S(f)$ and directional spreading function $G(\theta;f)$.

$$\Phi_{mn}(f) = \int_0^{2\pi} \exp[-ik\{(x_n - x_m)\cos\theta + (y_n - y_m)\sin\theta\}] S(f,\theta) d\theta \tag{4}$$

$$S(f,\theta) = S(f) \cdot G(\theta;f) \tag{5}$$

$$G(\theta) = \exp\left\{a_0 + \sum_{n=1}^{N} (a_n \cos n\theta + b_n \sin n\theta)\right\} \tag{6}$$

As the indicators of the wave spectrum shape, significant wave height $H_{1/3}$, mean wave period T_{01}, mean wave direction θ_m and mean spreading angle θ_k were estimated using moments of the frequency and directional spectrum. Here, mean wave direction represents a wave direction indicating the center of gravity of the directional spectrum, and mean spreading angle represents the dispersion of wave energy from the mean wave direction in the Cartesian coordinates of wavenumber domain.

Significant wave height and mean wave period are estimated using 0-th and 1-st order moment of the frequency spectrum as Eqs. (7) and (8), respectively. Here, the *n*-th order moment of the frequency spectrum is expressed as Eq. (9).

$$H_{1/3} = 4.0\sqrt{m_0} \tag{7}$$

$$T_{01} = \frac{m_0}{m_1} \tag{8}$$

$$m_n = \int_0^{f_{\max}} f^n S(f) df \tag{9}$$

In addition, mean wave direction and mean spreading angle are estimated as Eqs. (10) and (11) using the moment of the directional spectrum that is expressed in Eq. (12), respectively.

$$\theta_m = \tan^{-1} \frac{M_{01}}{M_{10}} \tag{10}$$

$$\theta_k = \tan^{-1} \frac{\sqrt{M_{00}}\sqrt{M_{01}^2 M_{20} - 2M_{10}M_{01}M_{11} + M_{10}^2 M_{02}}}{M_{10}^2 + M_{01}^2} \tag{11}$$

$$M_{pq} = \int_0^{f_{\max}} \int_{-\pi}^{\pi} S(f,\theta) k^{p+q} \cos^p \theta \sin^q \theta \, d\theta \, df \tag{12}$$

3.2 Analysis results of the experimental wave field

The estimated frequency spectra $S(f)$ and directional distributions of wave energy for each time interval are shown in Figure 3 (a) and (b), respectively. The directional distribution of wave energy is obtained by integrating the directional spectrum $S(f,\theta)$ with the frequency. The estimated frequency spectra and directional distributions of wave energy are in good agreement with the target values, and there is almost no temporal variation in both Figure 3 (a) and (b).

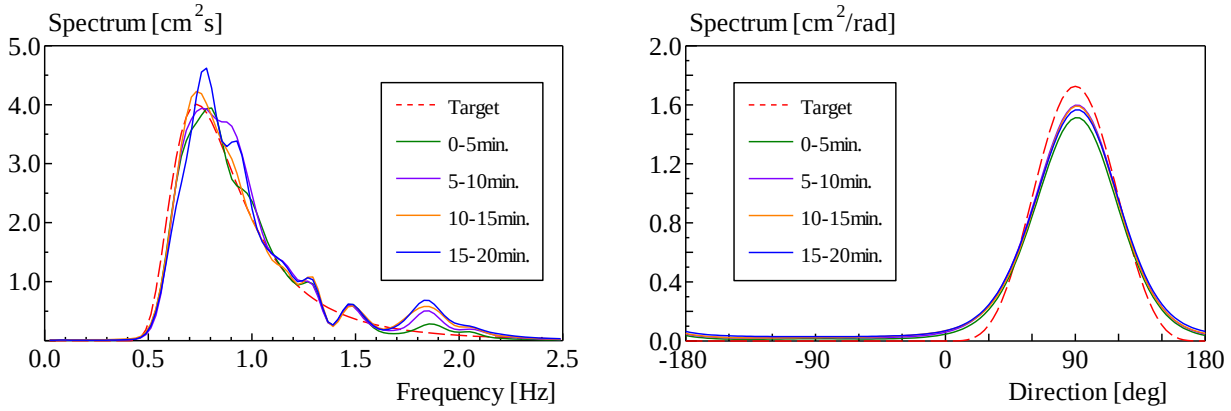

(a) Frequency spectra $S(f)$. (b) Directional distributions of wave energy.

Figure 3: Estimated frequency spectra and directional distributions of wave energy for each interval.

Figure 4 (a) ~ (d) shows the estimated directional spectra $S(f,\theta)$ for each time interval, which are represented with contour diagrams, and the color corresponds to the spectrum density. The target directional spectrum is shown in Figure 4 (e). As seen from Figure 4, the shapes of the estimated directional spectra for each time interval are in good agreement with the shape of the target directional spectrum. In addition, the principal wave direction and the peak frequency of the estimated directional spectra for each time interval are approximately consistent with the target values. Here, the target values of the principal wave direction θ_p and the peak frequency f_p are 90.0deg. and 0.73Hz, respectively.

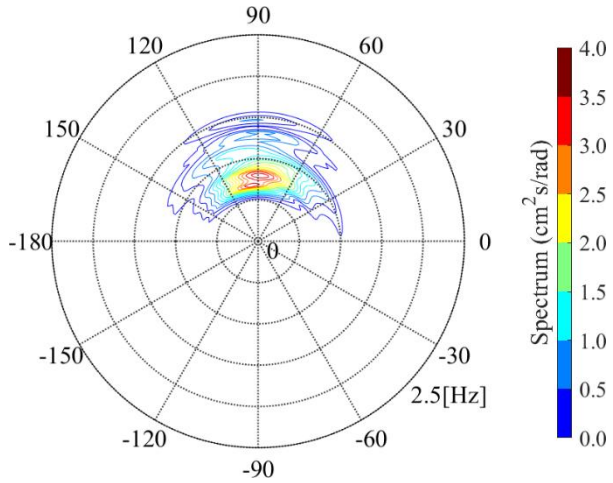

(a) Contour diagram of $S(f,\theta)$. (0-5min)

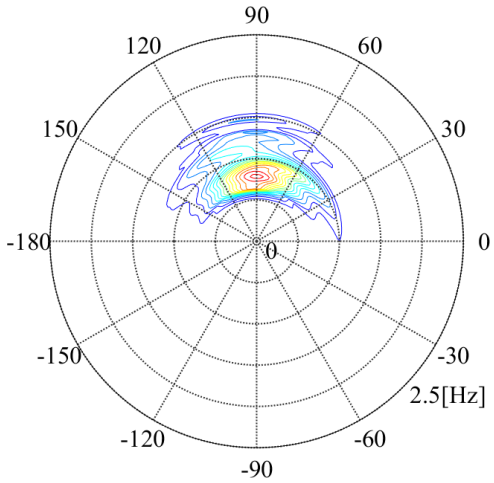

(b) Contour diagram of $S(f,\theta)$. (5-10min)

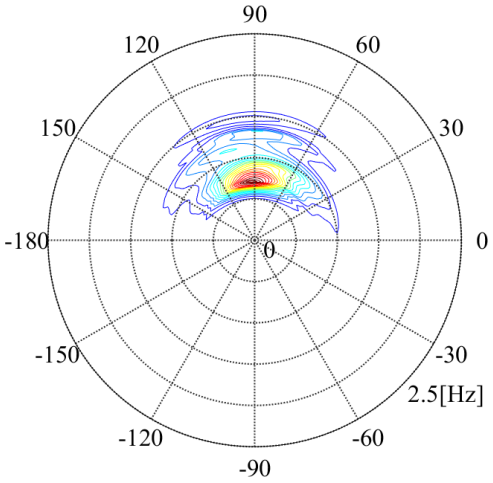

(c) Contour diagram of $S(f,\theta)$. (10-15min)

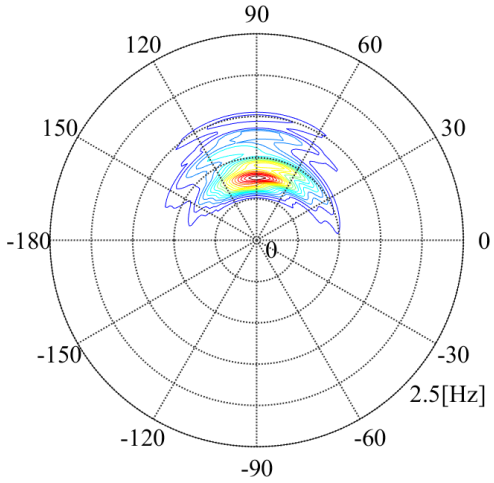

(d) Contour diagram of $S(f,\theta)$. (15-20min)

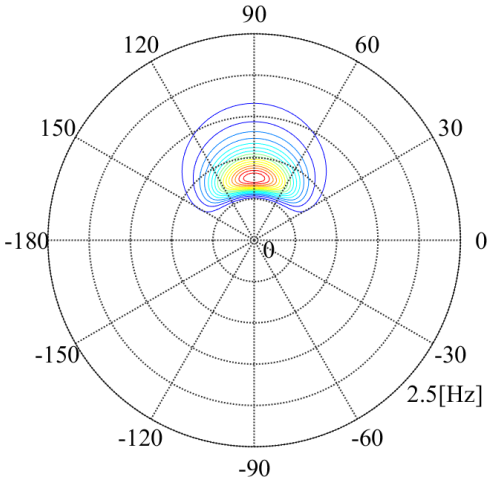

(e) Contour diagram of $S(f,\theta)$. (Target)

Figure 4: Contour diagrams of estimated directional spectra for each interval.

To quantify the temporal variation of the frequency spectrum, the significant wave height $H_{1/3}$ and the mean wave period T_{01} for each time interval are evaluated with the moments of the estimated frequency spectrum $S(f)$ as shown in Figure 5. In Figure 5 (a) and (b), the estimated values from the experimental wave field are plotted as blue circles, and the target values are represented as red lines. Both significant wave height and mean wave period are in good agreement with target values for each time interval. In addition, the standard deviation for four intervals of significant wave height is 0.12cm, and that of mean wave period is 0.02s. According to these results, there is almost no temporal variation in both parameters.

Furthermore, to quantify the directional properties of the wave fields, the temporal variation of the mean wave direction θ_m and the mean spreading angle θ_k are evaluated with the moments of the estimated directional spectrum $S(f,\theta)$ as shown in Figure 6 (a) and (b), respectively. As seen from Figure 6 (a), the mean wave directions for each interval are approximately consistent with the target value, and there is almost no temporal variation. Here, the standard deviation of the mean wave directions is 1.1deg. On the other hand, in Figure 6 (b), significant differences between the experimental mean spreading angles and the target value are observed. Moreover, the mean spreading angle increases as the wave generation time proceeds. Here, the standard deviation of the mean spreading angles is 4.1deg.

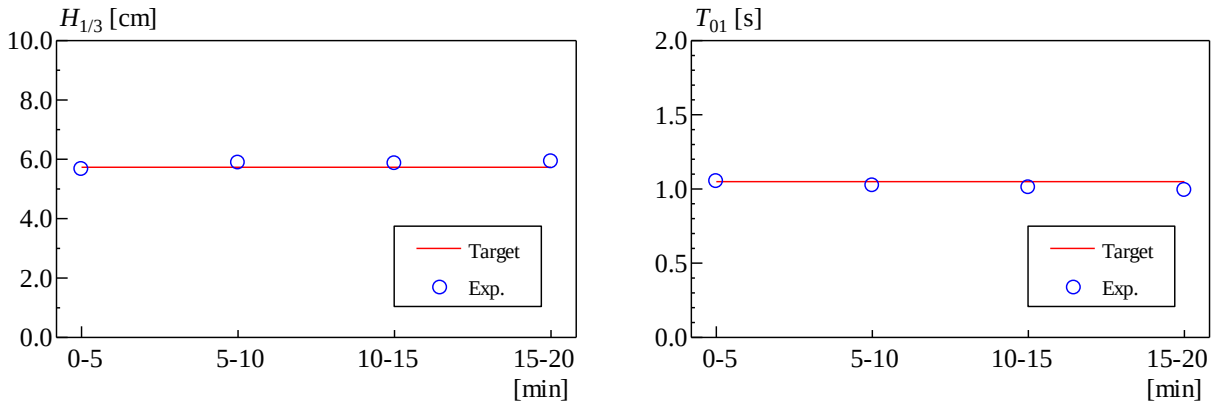

(a) Temporal variation of $H_{1/3}$. (b) Temporal variation of T_{01}.

Figure 5: Temporal variation of significant wave height $H_{1/3}$ and mean wave period T_{01}.

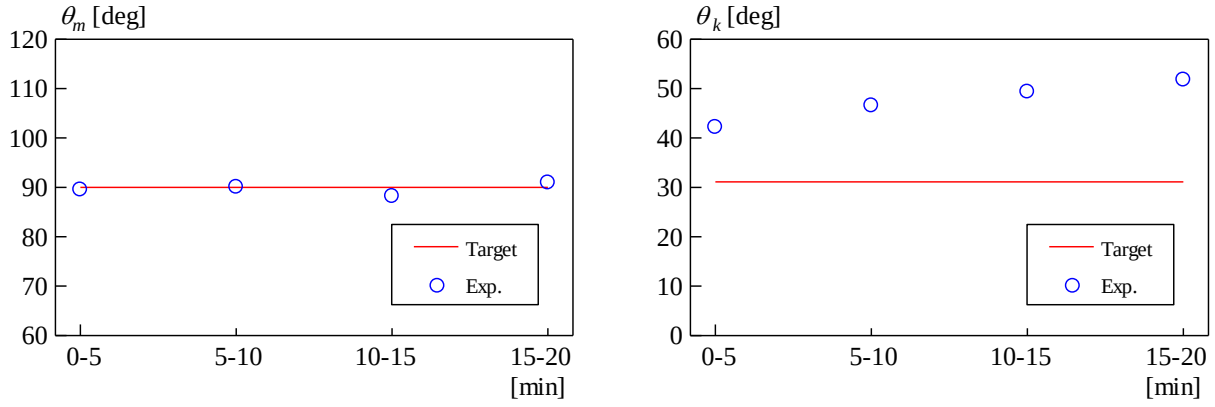

(a) Temporal variation of θ_m. (b) Temporal variation of θ_k.

Figure 6: Temporal variation of mean wave direction θ_m and mean spreading angle θ_k.

4 DISCUSSION ON THE INFLUENCE OF THE REFLECTED WAVES ON THE DIRECTIONAL SPECTRA

Temporal variations of the spectrum-shape indicators for the experimental wave field were evaluated, and it was revealed that mean spreading angle increases with wave generation time proceeds as mentioned in the previous section. The peak frequency can affect the mean spreading angle [4], but the peak frequency was almost unchanged in time in our experiment as shown in Figure 3. Therefore, in this section, we discuss the influence of the reflected waves on the estimation of the mean spreading angle with numerical wave fields. The wave reflection at the wave-makers occurs due to an imperfect absorption of incident waves.

The surface elevation of the wave field in which incident and reflected wave coexist is represented numerically by the summation of them as shown in Eq. (13).

$$\zeta(x,y,t) = \sum_{i}^{N} \{a_i \cos(k_i x \cos\theta_i + k_i y \sin\theta_i - 2\pi f_i t + \varepsilon_i) + r a_i \cos(k_i x \cos\theta_{ri} - k_i y \sin\theta_{ri} - 2\pi f_i t + \varepsilon_i)\} \tag{13}$$

In the right-hand side of Eq. (13), the first term in the summation represents the incident wave component, and the second term represents the reflected wave component. The value of r denotes the ratio of the amplitudes between the reflected and incident waves. Since the incident waves are reflected as specular reflection at the absorbing side of the basin, the reflected wave direction θ_{ri} coincide with the incident wave direction θ_i in Eq. (13). Note that the signs of the y-related terms of the incident and reflected waves are opposite because the mean wave direction coincides with the Y axis of the ASMB. The surface elevations with different r for 5-minutes interval were calculated, and the proposed indicators were estimated by spectral analysis. Figure 7 shows the contour diagram of the estimated directional spectrum with $r = 10\%$. The estimated directional spectrum is unimodal and approximately consistent with the experimental results shown in Figure 4 although the numerical wave field represented in Eq. (13) includes reflected waves whose peak direction is around -90deg. Figure 8 shows the variation of the proposed parameters as the reflectance r varies from 0% to 10%. Significant wave height appears to increase slightly with increasing the energy of the reflected wave, but there are almost no variation in mean wave period and mean wave direction. On the other hand, the mean spreading angle clearly increases with increasing reflectance. The present result suggests that the mean spreading angle in the experimental wave field increases in time due to the development of the reflected wave with the proceeding of the wave generation time.

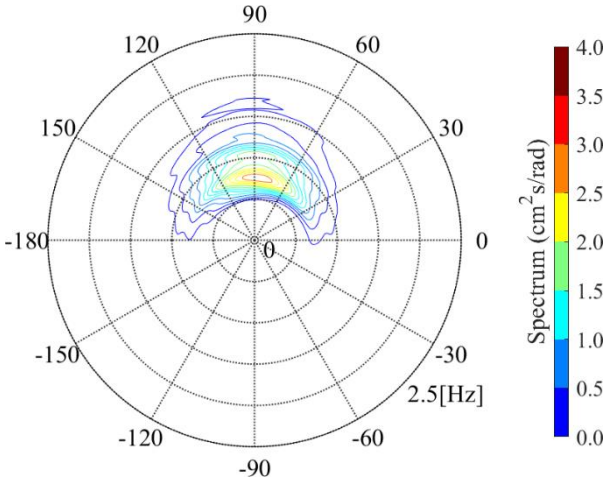

Figure 7: Contour diagram of estimated directional spectrum. ($r = 10\%$)

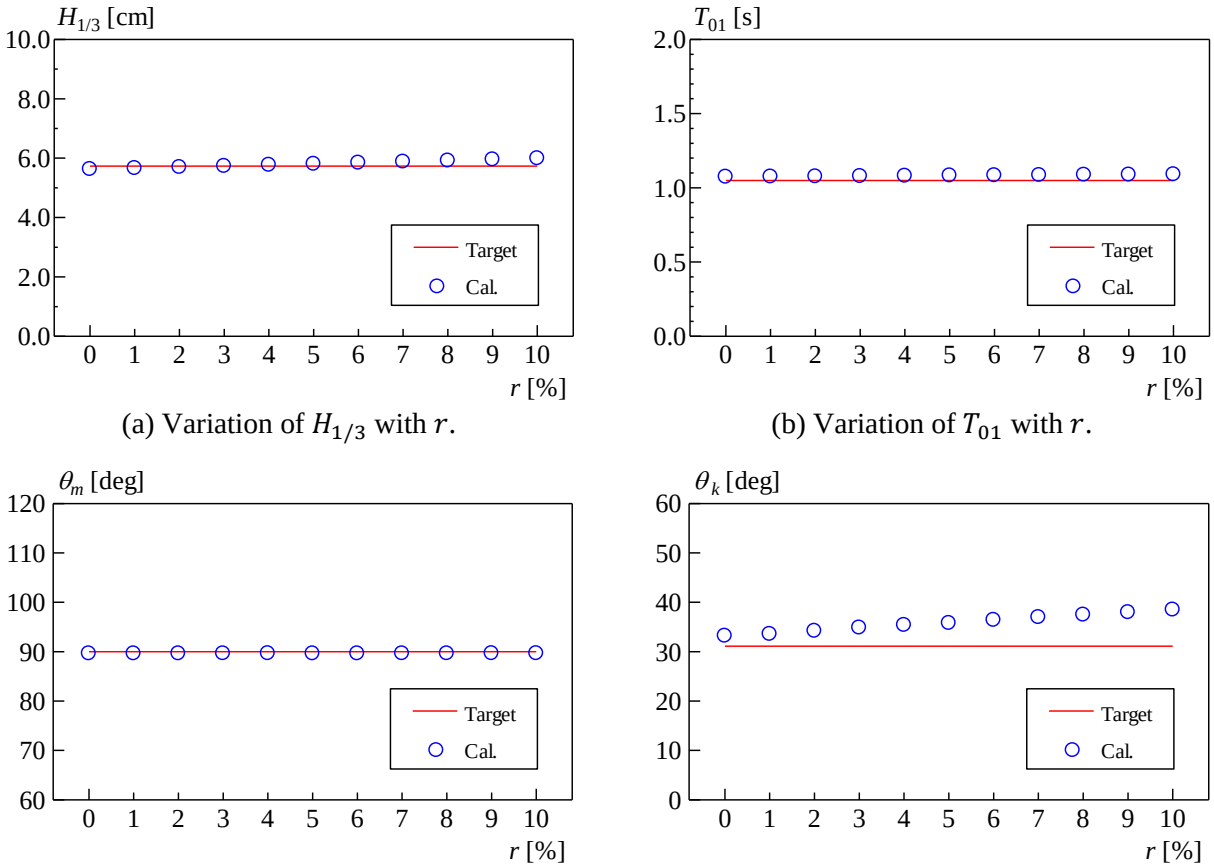

(a) Variation of $H_{1/3}$ with r.

(b) Variation of T_{01} with r.

(c) Variation of θ_m with r.

(d) Variation of θ_k with r.

Figure 8: Variation of indicator parameters with reflectance r.

5 CONCLUSION

The short-crested irregular wave was generated for 20-minutes in the ASMB, and the temporal variations of the spectrum-shape indicators for the experimental wave field were evaluated by spectral analysis. The introduction of these parameters allowed us to quantify the temporal variation of the directional irregular wave field generated in the wave basin. The analysis reveals the following:

1) The analysis of the frequency spectrum revealed that there is almost no temporal variation in the significant wave height and the mean wave period.
2) The analysis of the directional spectrum revealed that the mean wave direction has almost no temporal variation.
3) The mean spreading angle increases as the wave generation time proceeds.
4) By the numerical investigation, it was confirmed that the mean spreading angle increases due to the development of the reflected waves.

ACKNOWLEDGEMENTS

This study was carried out as a research activity of Goal-based Stability Criteria Project of Japan Ship Technology Association in the fiscal years of 2017, funded by the Nippon Foundation.

The authors created the analysis program using the EMEP method by reference to the program provided by Professor N. Hashimoto from Kyushu University in Japan.

REFERENCES

[1] Kuroda, T., Hara, S., Houtani, H. and Ota, D. "Direct Stability Assessment for Excessive Acceleration Failure Mode and Validation by Model Test". In: *Proc. of 13th International Conference on Stability of Ships and Ocean Vehicles*, Kobe, Japan, 2018.

[2] Maeda, K., Hosotani, N., Tamura, K. and Ando, H. "Wave Making Properties of Circular Basin". In: *International Symposium on Underwater Technology*, 349-354, 2004.

[3] Tsujimoto, M., Kuroda, M., Shiraishi, K., Ichinose, Y. and Sogihara, N. "Verification on the Resistance Test in Waves Using the Actual Sea Model Basin". In: *Journal of the Japan Society of Naval Architects and Ocean Engineers*, Vol. 16, 33-39, 2012.

[4] Goda, Y. "Random seas and design of maritime structures (3rd edition)". World Scientific, 2010.

[5] Hashimoto, N., Nagai, T. and Asai, T. "Extension of the Maximum Entropy Principle Method for Directional Wave Spectrum Estimation". In: *Proc. of 24th Conference on Coastal Engineering*, Kobe, Japan, 232-246, 1994.

[6] Isobe, M., Kondo, K. and Horikawa, K. "Extension of MLM for estimating directional wave spectrum". In: *Proc. of Symp. on Description and Modeling of Directional Seas*, Copenhagen, Denmark, A-6-1 - A-6-15, 1984.